Time and Space Structure of Interannual Variations in Summer Rainfall over China

By Shao-Fen Tian

Environmental Research Center, University of Tsukuba, Ibaraki 305, Japan

and

Tetsuzo Yasunari

Institute of Geoscience, University of Tsukuba, Ibaraki 305, Japan
(Manuscript received 15 July 1991, in revised form 10 December 1991)

Abstract

The time and space structure of interannual fluctuations of summer rainfall (May to September) for the period from 1951 to 1990 over China is described. First, a harmonic analysis is applied to the summer rainfall series. The variation with periods of two to four years (hereafter, refered to 2–4 year component) accounts for more than 40 percent of the total variance for all stations, and more than 70 percent of the total variance for 61 percent of stations. The three-year period seems most prevailent among this period band.

An EOF (Empirical Orthogonal Function) technique is applied to the 2–4 year period series. The first two EOF modes account for 12.8 and 10.7 percent of the total variance, respectively. EOF mode 1 reveals the seesaw between the Yangtze River valley and the Northern part of China. The spatial pattern of EOF mode 2 is more complicated, but it may be characterized by the oscillation between the Mei-yu region including the Yangtze River valley, and the rest of the country. Although the contribution proportion of the two principle modes is not high, composite maps show that they present the situations (before applying the EOF analysis) well. These two EOF modes exhibit large amplitude modulations. The amplitudes or the squares of the time coefficients tend to become large or small alternatively.

Correlation and composite analyses show that EOF mode 1 correlates with the Indian summer monsoon and the SOI (Southern Oscillation Index). This result agrees with that of preceding studies and suggests that the summer rainfall over China is associated with the ENSO (El Nino and Southern Oscillation) events on the time-scale of two to four years. EOF mode 1 seems to precede the anomaly of the SOI. This result supports the previous proposals that the ENSO signals in the eastern equatorial Pacific may originate in the central Asia or the Indian Ocean region. EOF mode 2 seems not to be related to the Indian monsoon and the ENSO.

1. Introduction

Previous observational studies have described interannual fluctuations in rainfall in China (for example, see Wang and Zhao, 1981). Xu and Dong (1982) found a quasi-three-year period oscillation in the precipitation over the western part of China. Furthermore, Zhao (1986) demonstrated that a quasi-biennial oscillation prevails in the eastern part of China, while a quasi-three-year oscillation prevails in the western part. Many researches indicated that there exist some links between several indices of atmospheric circulation and interannual variations of rainfall over some regions in China. For instance, Sha and Li (1979) found that fluctuations in rainfall over the lower Yangtze River valley are influenced by the subtropical high and SST (Sea Surface Temperature) in the Pacific Ocean. Recently, the influences of ENSO (El Nino and Southern Oscillation) on rainfalls over China have been noted. Huang and Wu (1987) found that rainfall over China is significantly influenced by the SST in the eastern equatorial Pacific. Wang and Li (1990) demonstrated that the precipitation fluctuation over the semi-arid region of northern China exhibits a 2–3 year oscillation and is significantly linked with the ENSO events. However, there have been fewer investiga-

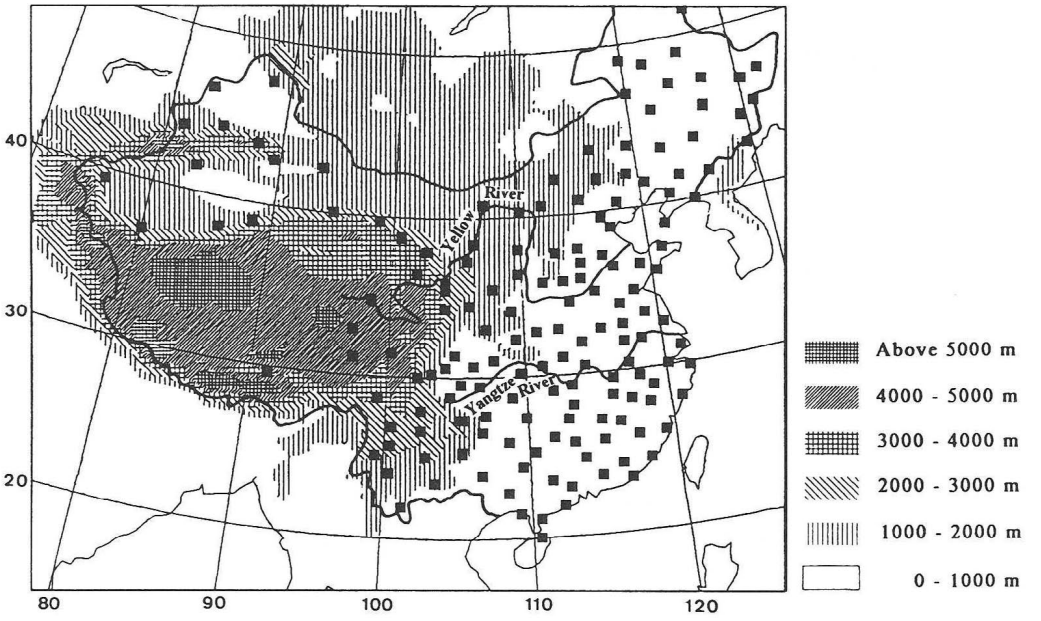

Fig. 1. Geographical distribution of the observation stations. Altitudes averaged on a box of 1 degree latitude by 1 degree longitude are superposed.

tions so far on the interannual variations over the whole of China. The purpose of the present study is to acquire a basic understanding of the time and space structure of the interannual variations of the rainfall over the whole of China. The associations with the ENSO and the Indian summer monsoon are also discussed.

Since a considerable amount of rainfall is concentrated in the Asian summer monsoon period, that is, in the summer half of the year in China (Xu *et al.*, 1983; Yoshino and Chiba, 1984), we discuss only the summer monsoon rainfall. In the present study the summer rainfall is defined as the total amount of rainfall during the five months from May to September.

2. Data

The monthly precipitation dataset for 160 stations compiled by the State Meteorological Bureau of China is used in this study. The dataset covers a period of 40 years from 1951 to 1985. The geographical distribution of the stations is shown in Fig. 1. Generally, the observation station network is dense in the eastern part but it is sparse in the western part. Only a few stations are located over the Tibetan Plateau. Figure 2 shows the distribution of the mean over the 40 years of summer rainfall. Much summer rainfall occurs in the southeast part and gradually decreases toward the northwest part. Figure 3 shows the ratio of the standard deviation to the mean, which is nearly the reversed pattern of Fig. 2. The year-to-year variability is larger in the northwest part and smaller in the southeast part. On the northern foot of the Tibetan Plateau the

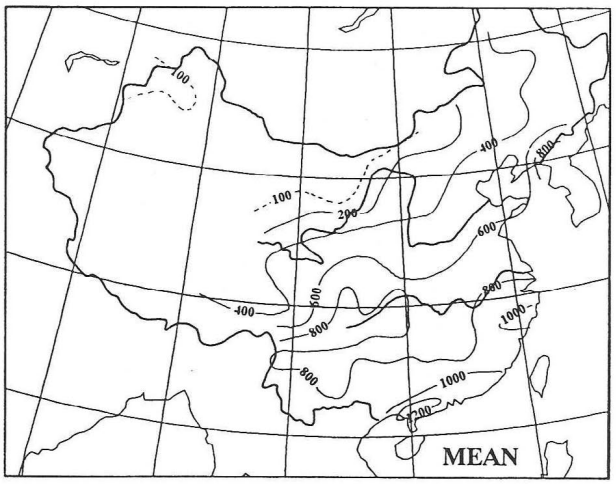

Fig. 2. Spatial distribution of the long-term mean of summer rainfall (in mm).

standard deviation is comparable to the mean. The year-to-year variability is smaller also in the northeast part.

3. Harmonic analysis

We assume that the series of the summer rainfall at each station is described by:

$$P(t) = p_0 + \sum_{k=1}^{N/2} p_k(t)$$

Where p_0 is the long-term mean, t the time in years, N the data length in years, (equals 40 years), $p_k(t)$ the k-th harmonic component, given by:

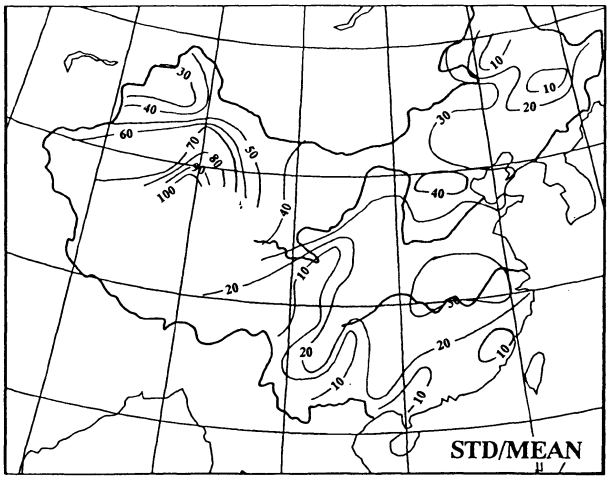

Fig. 3. Spatial distribution of the ratio of the standard deviation to the mean for summer rainfall.

$$p_k(t) = a_k \cos kt + b_k \sin kt,$$

where a_k, b_k, are the coefficients for the k-th harmonic component. Since our interest is mainly in variations on the interannual time scale, we eliminate variations longer than 10 years by subtracting the long-term mean and the first four harmonic components. Then the variations with periods shorter than 10 years are described by:

$$\tilde{P}(t) = \sum_{k=5}^{N/2} p_k(t)$$

To examine how the rainfall belts oscillate spatially, we use the relative values or the normalized series $X(t)$ instead of the absolute rainfall series $\tilde{P}(t)$:

$$X(t) = \sum_{k=5}^{N/2} x_k(t)$$

$$x_k(t) = p_k(t)/\sqrt{\sigma}.$$

σ is the total variance of $\tilde{P}(t)$:

$$\sigma = \frac{1}{2} \sum_{k=5}^{N/2} \left(a_k^2 + b_k^2\right).$$

If we round the period T/k for the k-th harmonic component to the nearest integer number and reconstruct components for periods with two, three, four and five to nine years by summing up the harmonic components with the same integer period band, respectively, then:

$$\hat{X}_2(t) = \sum_{k=17}^{20} x_k(t)$$

$$\hat{X}_3(t) = \sum_{k=12}^{16} x_k(t)$$

$$\hat{X}_4(t) = \sum_{k=9}^{11} x_k(t)$$

$$\hat{X}_{5-9}(t) = \sum_{k=5}^{8} x_k(t).$$

Figure 4 shows spatial distributions of the variances for $\hat{X}_2(t)$, $\hat{X}_3(t)$ and $\hat{X}_4(t)$ at each station. The most outstanding feature may be that the variance contributed by the three-year-period component is much larger than the other two period bands for most stations. The variance of the two-year-period variation is relatively larger in the northwest part, the Yangtze River valley, the southeast coastal region and the southwest part, but it seems to be smaller in the northeast part, the upper and the middle reaches of the Yellow River valley. From Fig. 4b, and we can see that the three-year-period component is the most predominant in the Yellow River valley, the northeast part, and the southwest part. Larger variances can also be found in regions to the south of the Yangtze River. For four-year period variations, relatively large variance appears in the region from the northeast part to the lower Yellow River, regions between the upper Yellow River and the upper Yangtze River, and the northwest part of China.

The predominance of the three-year and the two-year periods is similar to the result of the spectral analysis by Zhao (1986). He also concluded that periods of 21.2–29.2 months and 31.4–39.0 months are predominant in the monthly precipitation of China. There are, however, some differences between his result and ours. In his study the magnitudes of the two oscillations were nearly comparable, while, in ours, the amplitudes or variances of three-year period are generally larger than for the two-year period. In the northeast of China the quasi-biennial oscillation is dominant in his analysis, but the variation of three-year period is more remarkable in ours. This inconsistency may be due to the differences in the datasets. The datasets used in both studies are fundamentally the same, but ours is 10 years longer than his. Furthermore, we adopted summer rainfall here, while, in his analysis, the monthly mean was used.

The variances accounted for by components with periods of two to four years $\sum_{m=2}^{4} \hat{X}_m(t)$ and five to nine years $\hat{X}_{5-9}(t)$ are plotted in Fig. 5 (Hereafter referred to 2–4-year and 5–9-year components). The 2–4 year component accounts for more than 40 percent of the total variance in all stations, and more than 70 percent of the total variance for 61 percent of stations. Therefore the 2–4 year component is

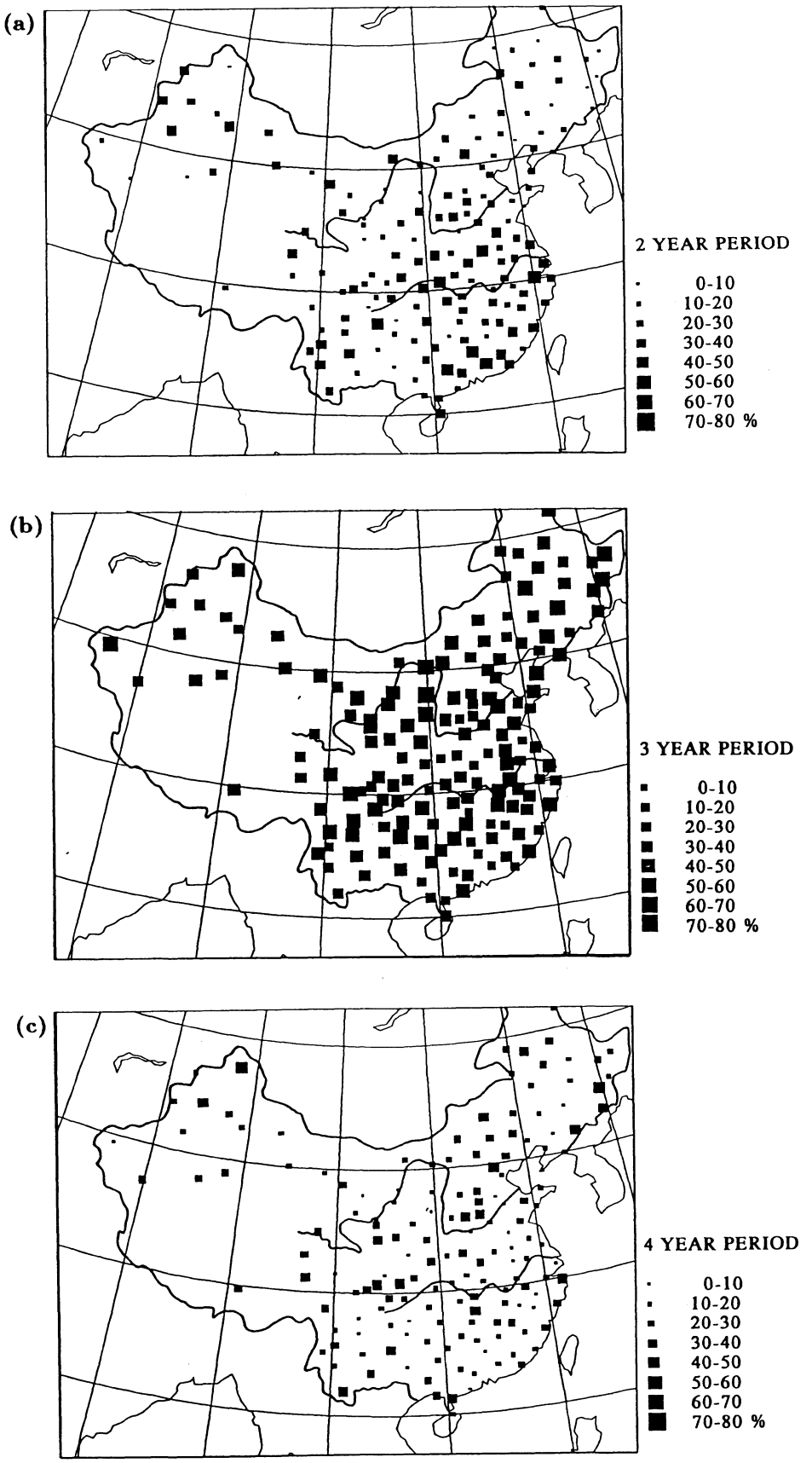

Fig. 4. Spatial distributions of variance contributed by each period band (in percentage), (a) for two years, (b) for three years and (c) for four years.

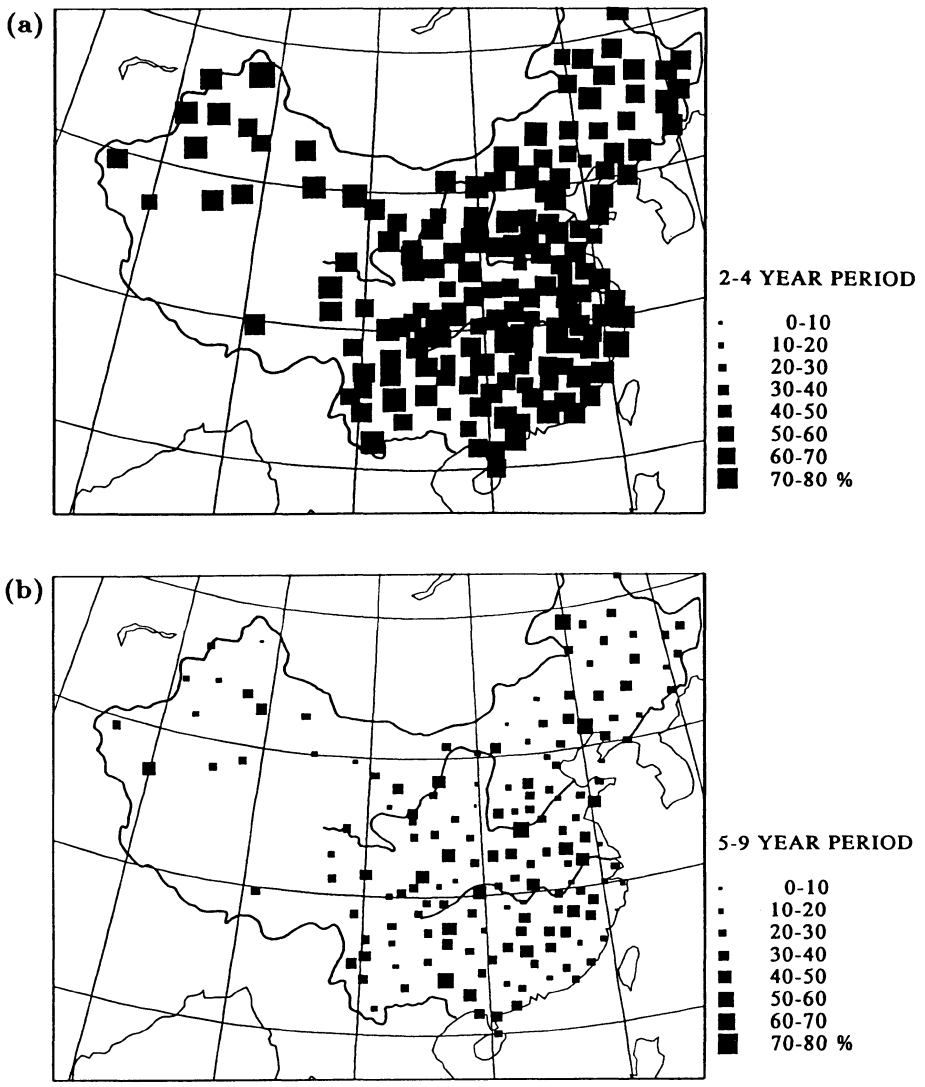

Fig. 5. Same as Fig. 2 excepting (a) for the 2–4 year period band, (b) for the 5–9 year band.

considered as representative of the variations of the of summer rainfall on the interannual time-scale and we only discuss it below.

4. Time-space structure of the 2–4-year period oscillation

To explore the time-space structure of the predominant mode of interannual rainfall fluctuation over the whole of the country, an EOF (Empirical Orthogonal Function) analysis is applied to the reconstructed series of the 2–4-year component. Here, the correlation matrix is used for calculating the eigenvalues and eigenvectors.

The spatial distributions of amplitudes of the first two EOF modes are indicated in Fig. 6. The first two EOF modes account for 12.8 and 10.7 percent of the total variance, respectively. Considering the fact that theoretically we should use 160 EOF components to account for the total variance, and we have a very small observation number (40 observations) compared with the variable number (160 variables or stations), the proportions contributed by the first two modes are not so small. Figure 6a shows that a broad area with large positive deviation extends from north China to the northwest part in EOF mode 1. A narrow band with negative deviation is elongated along the Yangtze River. The region to the south of the Yangtze River exhibits a moderately positive deviation. A negative deviation area also appears in northeast China. This mode corresponds to a situation when the time coefficient is positive/negative then the convection is suppressed/enhanced over the Yangtze River Valley, and the most northeast part and enhanced/suppressed over the rest. The spatial pattern of this mode closely resembles that of Huang and Wu (1987) but with the reversed sign; however, they were correlating the summer rainfall with the SST in the eastern equatorial Pacific.

Compared with EOF mode 1, the spatial pattern

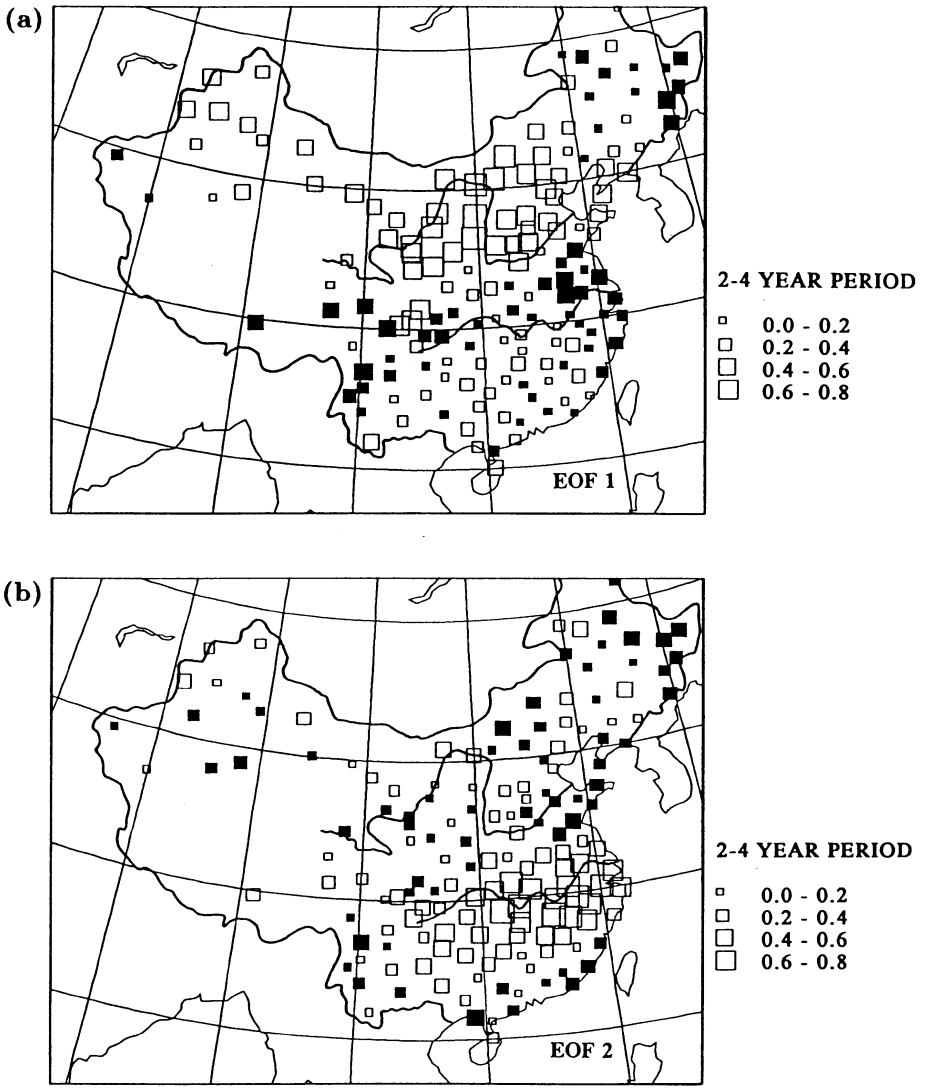

Fig. 6. Spatial pattern or amplitude distribution at each station for (a) EOF mode 1 and (b) EOF mode 2 in relative units. This Unit, when multiplied with the that of time coefficients in Fig. 7, gives the ratio to the standard deviation of the 2–4 year series. Open and black squares indicate positive and negative values, respectively.

of EOF mode 2 (Fig. 6b) is more complicated. This mode, however, seems to show a seesaw between the Mei-yu region broadly distributed in the Yangtze River valley and the rest of the country. When the time coefficient is positive/negative then the convection is enhanced/suppressed over the Mei-yu region but suppressed/enhanced over the rest.

The time series, or time coefficients, of the first two EOF modes are shown in Fig. 7. Both modes show great amplitude modulations. EOF mode 1 shows a larger amplitude during the period from the late 1950s to late 1960s and the end of the 1980s, while smaller in the early 1950s and during the period from the end of the 1960s to the middle 1980s. EOF mode 2 has its larger amplitudes during the first half of the 1950s and the period from the late 1960s to the beginning of the 1980s, and its smaller amplitudes in the late 1950s and 1980s. This relativities are better seen from Fig. 8. When the amplitude, or the square of the time coefficient, of mode 1 is larger, that of mode 2 is smaller and *vice versa*, excepting for the years, *e.g.* 1963, 1968, 1972, 1973, 1980 and 1981. In other words, the two modes tend to prevail alternatively.

In order to examine how the dominant EOF modes represent the observed anomalies we produced the composite of normalized, trend-removed summer rainfall $X(t)$ for the two modes (Fig. 9). Before producing the differential composite for the positive and negative time coefficients, we have composited the positive and negative cases separately. They show nearly the same patterns but with reversed signs (not shown). We notice that the composite patterns resemble those of the two EOF modes. This

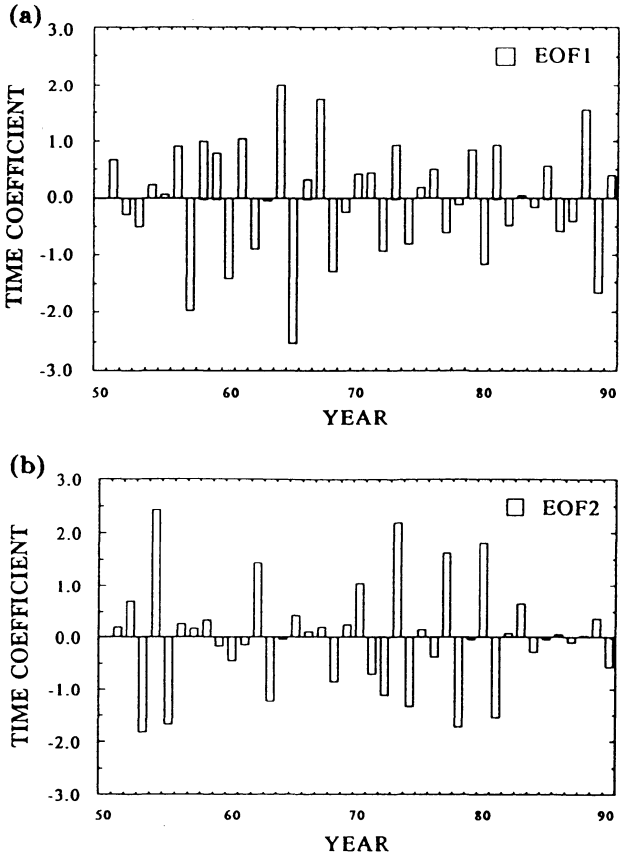

Fig. 7. Time series or time coefficients for EOF modes 1(a) and 2(b).

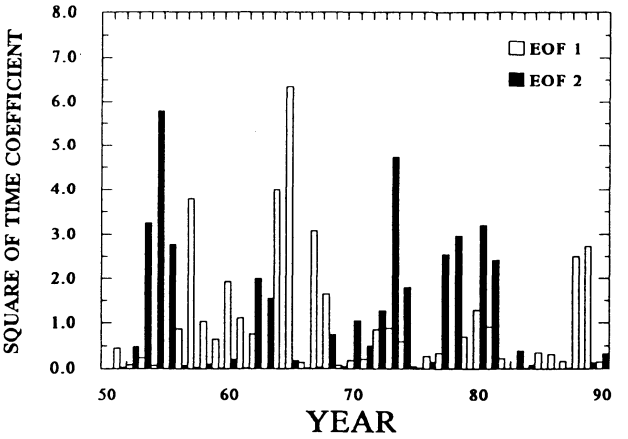

Fig. 8. Square of the time coefficients of EOF modes 1 and 2.

result suggests that the two EOF modes reflect the situations before applying the EOF analysis well. Considering together the relationship between the amplitudes of the two EOF modes shown in Fig. 8, we can conclude that the two modes prevail alternatively, rather than appear simultaneously.

Since the summer rainfall in China is basically subject to the Asian monsoon circulation system, we compared the time series of the principal modes derived above to the Indian monsoon rainfall index (IMR). The IMR is adopted from Parthasarathy (1987) and is defined as the area-averaged total precipitation from June to September over the whole of India (for details see Parthasarathy and Mooley, 1978). Fluctuations with periods longer than 10 years involved in the IMR are removed and the series obtained is then normalized. The time series of the IMR with a period of two to four years is prepared by the same procedure as for the China summer rainfall. Figure 10 shows the series of the IMR with the time series of EOF modes 1(a) and 2(b) superposed. EOF mode 1 is generally correlated well with the Indian monsoon rainfall, while EOF mode 2 does not exhibit a consistent relation. To examine this further we calculated the lag correlation between the IMR and the time coefficients of the two EOF modes. It is difficult to estimate the significance level because the both series are performed with the same filter and the effective freedom number can not easily be decided. However, from Table 1 we can see that EOF mode 1 is most strongly correlated with the IMR simultaneously with a correlation coefficient of 0.45. Negative correlations are also found when EOF mode 1 preceeds or lags the IMR by one year, but not equally. This result is explained by the fact that the periodicity of two to four years is dominant, but it is not exactly two years. Compared with EOF mode 1, the correlations between EOF mode 2 and the IMR are much smaller, and barely reaches -0.29 when the EOF mode 2 lags the IMR by one year. This result suggests that EOF mode 1 is associated with the Indian monsoon, while EOF mode 2 does not have a consistent relationship with it.

Furthermore, the relationships of the two principle modes to ENSO are also examined. We compared the time series of the two modes with that of the SOI (Southern Oscillation Index), an indicator of ENSO. Here the SOI is defined as the difference of the monthly mean of the SLP (Sea Level Pressure) at Tahiti and Darwin. The time series of the SOI used here is also normalized and performed by a band-pass filter, which is developed by Murakami (1979), with 0.5 response at 18 and 50 months, and 1.0 response at 30 months. Figure 11a shows that mode 1 exhibits a good correspondence with the SOI. Mode 1 tends to reach the extremes several months to a half year in advance of the SOI. From Fig. 11b, however, mode 2 does not show a consistent relationship with the SOI. To further comfirm this relationship, we composite the anomaly of the SOI of each three successive years referenced to the time series of the two EOF modes. The SOI reaches its maximum in September of the reference year, lagging the EOF mode 1 by a month (shown by the solid line) and reaches its minimum in the following January (shown by the dashed line), lagged the

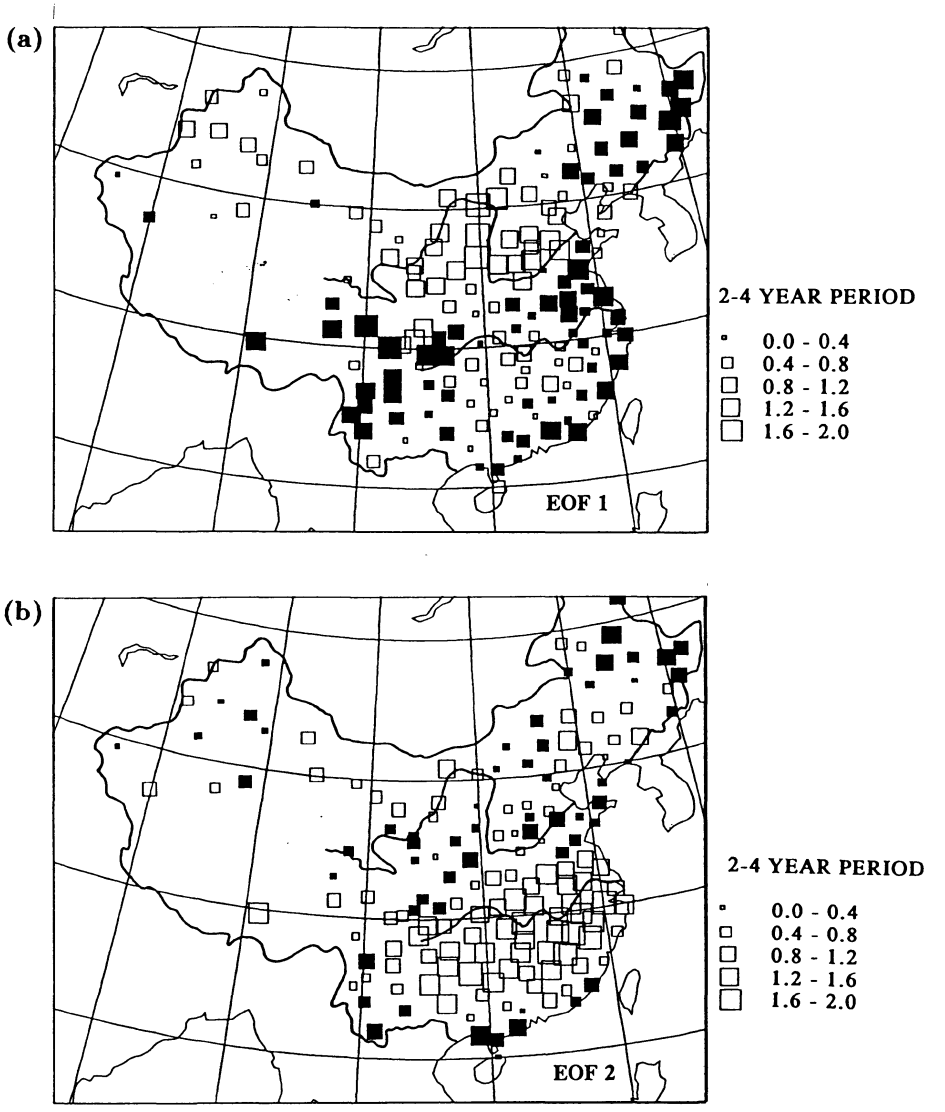

Fig. 9. Differential composite of the normalized, trend-removed summer rainfall $X(t)$ or the mean of all $X(t)^+$ and $-X(t)^-$. $X(t)^+$ and $X(t)^-$ denote the values of $X(t)$ when the time coefficient of EOF modes 1(a) or 2(b) is above +1.0 and below −1.0, respectively. Open and black squares indicate positive and negative values, respectively.

EOF mode 1 by a half year (Fig. 12). The composite of the SOI shows a nearly inverse anomaly when the time coefficient of EOF mode 1 takes the opposite signs. This result is essentially consistent with the finding by Huang and Wu (1987). They reported that in the summers of the developing stage of El Niño, floods occur in the Yangtze River and Huaihe River valleys, and droughts occur in the Yellow River valley. Additionally, by comparing the spatial patterns, we can conclude that our EOF mode 1 is basically identical with the correlation pattern of Huang and Wu (1987), and it is associated with the ENSO events. It is noteworthy that the composite of the SOI shows reversed signs in the previous and the following years referenced to the years when the EOF mode 1 reaches is extremes. This fact is also explained by the periodicity of two to four years. However, although the composite of the SOI by the EOF mode 2 reaches its maximum of 0.32 in the January of the previous year, falls and then turns rapidly negative, no significant difference is found when the EOF mode 2 changes its sign. It seems that the EOF mode 2 does not have a consistent relationship with the SOI.

5. Discussion

As described above, our EOF mode 1 is essentially identical with the correlation pattern of Huang and Wu (1987), and is associated with the El Niño events. From the present and previous studies there is no doubt that the Asian monsoon circulation including the Indian summer monsoon, the summer rainfall over China, and the ENSO events are coupled on the 2–4 year time scale. From the analy-

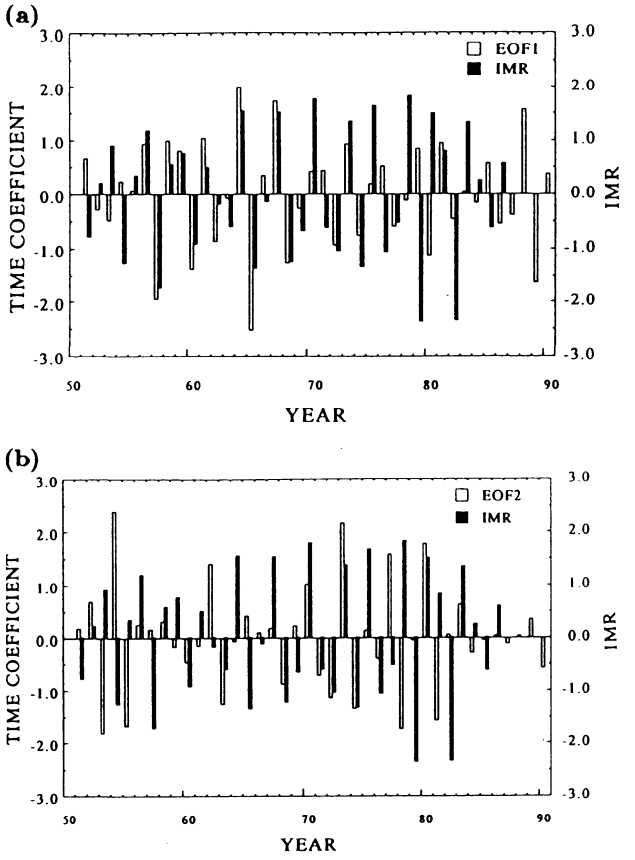

Fig. 10. Time sequences of the Indian monsoon rainfall index (measured by the standard deviation) with that of (a) EOF mode 1 and (b) EOF mode 2 superimposed.

sis of the global SLP using a complex EOF technique, Barnett (1985) proposed that large SLP signals associated with the Southern Oscillation and monsoon may have their origin in a SLP/snow feedback loop that acts over the region from Siberia to India. Yasunari (1987) also found that the significant ENSO-associated signals in the SLP first appear over the Indian Ocean, and seem to originate from central Asia or Eurasia. Recently, from extensive comparison of the Indian monsoon, SWT (Sea Water Temperature) in the Western Pacific and the SOI, Yasunari (1990) suggested that the Asian monsoon may have an active role rather than a passive role in the interannual variability, including the ENSO events, of the coupled atmosphere/ocean system over the tropical Pacific. Huang and Wu (1987) emphasized the influence of the ENSO events in the explanation of the association between the summer rainfall over China and ENSO events. We also consider that the Asian monsoon circulation is coupled with the ENSO, but it may be more rational to consider that anomalies in the Asian monsoon circulation lead the ENSO events and may be a trigger for them. In fact, Huang and Wu (1987) also indicated that the summer rainfall is strongly correlated with

Table 1. Lag correlations between IMR and the time coefficients of EOF modes 1 and 2. Lags −1 and +1 indicate that the IMR preceeds and lags the time coefficients, respectively, by one year.

Lag	EOF1	EOF2
−1	−0.34	0.13
0	0.45	0.07
+1	−0.18	−0.29

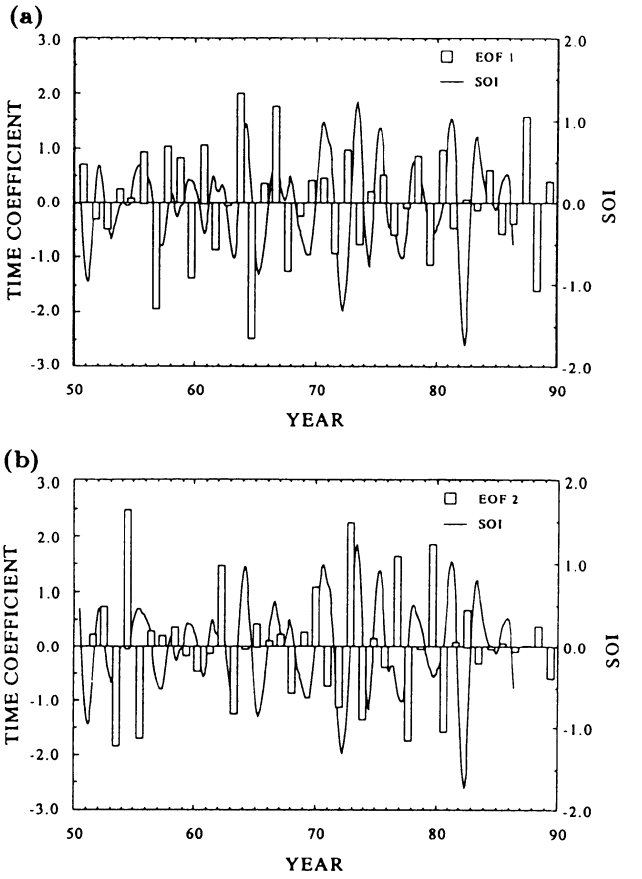

Fig. 11. Same as Fig. 9 excepting for the SOI (measured by the standard deviation).

the SST in the eastern equatorial Pacific in the developing stage of the ENSO events. Further evidence may be found from the result of Meehl (1987). He introduced a concept of a strong/weak monsoon year, and showed a dynamically coupled ocean-atmosphere system in the Indian-Pacific region to be involved in producing Southern Oscillation-type signals in the atmosphere and ocean in these sets of years, with extremes in the system being manifested as Warm and Cold events. In other words, after a strong/weak monsoon, a Cold/Warm event may have a large chance of subequently occurring, but this does not always happen. It is considered that in strong Indian monsoon years, Hadley circu-

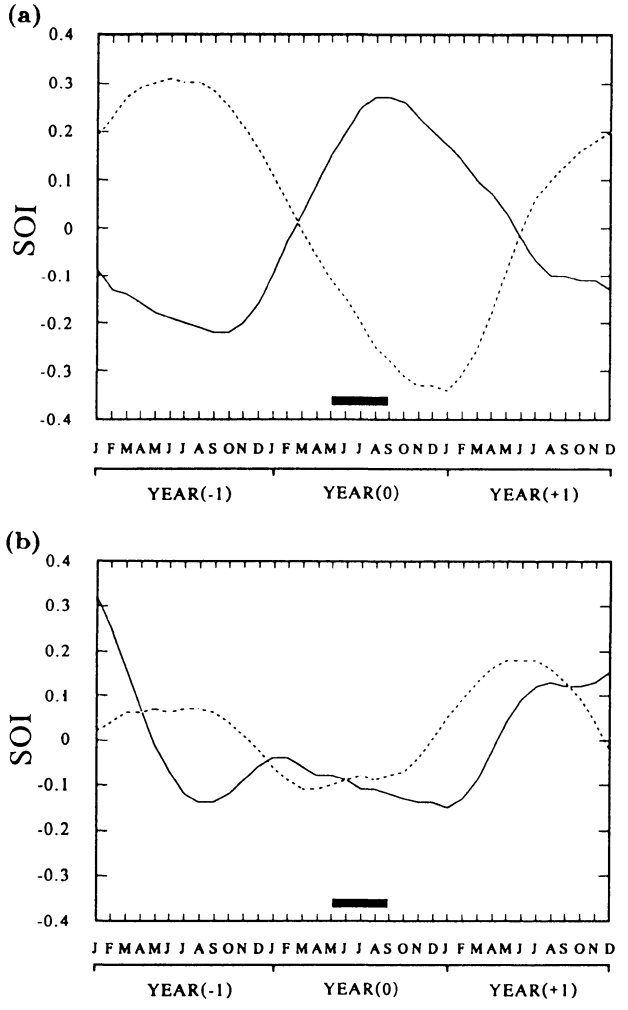

Fig. 12. Composite of SOI by the time coefficients of EOF modes 1(a) and 2(b) (Measured by the standard deviation). Solid and dashed lines are the composites when the time coefficient is above +1.0 and below −1.0, respectively. The Black thick bar indicates the referenced summer rainfall period in China. YEAR (−1), YEAR (0) and YEAR (+1) denote the previous, referenced and following years, respectively.

lation over the western Pacific sector is stronger than normal because of the enhanced convection over the western equatorial Pacific. This condition induces the rainbelt over the Yangtze River Valley to shift northward. As a result, the Yangtze River Valley region undergoes a drought, and most of north China, and the coastal region of the southeast part undergo a wet condition. This situation corresponds to the positive extremes of the EOF mode 1 and possibly is followed by a cold event. The opposite situation takes place when the time coefficient of the EOF mode 1 reaches the negative extreme.The positive anomaly over the southeast part maybe partly due to the increased autumn typhoon visits. Further analysis based on shorter monthly data is necessary to confirm it.

EOF mode 2, however, does not show a consistent relationship with the Indian monsoon and the ENSO event. Further analyses are necessary to clarify the physical background when this mode is dominant. At least, we have been successful in exploring a significant mode which seems not be associated with the ENSO events. However, this mode cannot be deduced by the correlation analysis method or the composite technique by referring to the the ENSO events.

The rainbelt appears in the southeast China in May and migrates northward gradually, reaches to the north and northeast part in late July or early August and then retreats (*e.g.* see Xu *et al.*, 1983). There is no doubt that different spatial patterns of the summer monsoon rainfall are associated with differences in the seasonal march of the rainbelt from year to year. It remains an unsolved question as to how the seasonal march of the rainbelt, including the intraseasonal oscillation, changes from year to year. We will discuss this problem in a later paper.

6. Conclusions

Time and space structure of interannual fluctuations of summer rainfall was described by applying a harmonic analysis technique and an EOF (Empirical Orthogonal Function) to the summer rainfall (May to September) series of 40 years from 1951 to 1990 for 160 stations in China. Additionally, the relationship of two principal EOF modes to the Indian summer monsoon rainfall and the SOI (Southern Oscillation Index) were discussed. The main results of this study are summarized as follows:

1. The harmonic analysis indicates that variation with periods of two to four years (the 2–4 component) accounts for more than 40 percent of the total variance at all stations, and more than 70 percent of the total variance for 61 percent of stations. The three-year period prevails most among this period band.
2. EOF mode 1, which accounts for 12.8 percent of the total variance, reveals the seesaw between the Yangtze River valley and the Northern part of China.
3. EOF mode 2 which, accounts for 10.7 percent of the total variance, seems more complicated. However, it may be characterized by the oscillation between the Mei-yu region including the Yangtze River valley and the rest of the country.
4. These two EOF modes exhibit large amplitude modulations. The amplitudes or the squares of the time coefficients tend to become large alternatively.

5. EOF mode 1 shows good correspondence with the Indian summer monsoon and the SOI (Southern Oscillation Index). This result agrees with that of preceding studies and suggests that the summer rainfall over China is associated with ENSO events on a time-scale of 2–4 years (*e.g.*, Huang and Wu, 1987).
6. Furthermore, EOF mode 1 seems to precede the anomaly of the SOI. This supports the previous proposals (Barnett, 1985; Yasunari, 1987) that the ENSO signals in the eastern equatorial Pacific may originate in central Asia or the Indian Ocean region.
7. EOF mode 2 seems not to be related to the Indian monsoon or the ENSO.

Acknowledgements

The authors would like to thank Miss A. Yatagai for the assistance in preparing the figures.

References

Barnett, T.P., 1985: Variations in near-global sea level pressure. *J. Atoms. Sci.*, **42**, 478–501.

Huang, R.-H. and Y.-F. Wu, 1987: The influence of the ENSO on the summer climate change in China and its mechanism. *Japan-U.S. workshop on the El Nino Southern Oscillation Phenomenon, November 3–7, 1987, Tokyo, Japan.*

Meehl, G.A., 1987: The annual cycle and interannual variability in the tropical Pacific and Indian Ocean regions. *Mon. Wea. Rev.*, **115**, 27–50.

Murakami, M., 1979: Large-scale aspects of deep convective activity over the GATE area. *Mon. Wea. Rev.*, **107**, 994–1013.

Parthasarathy, B., 1987: Droughts/floods n the summer monsoon season over different meteorological subdivision of India for the period 1871–1984. *J. Climatol.*, **7**, 57–70.

Parthasarathy, B. and Mooley D.A., 1978: Some features of a long homogeneous series of Indian summer monsoon rainfall. *Mon. Wea. Rev.*, **106**, 771–781.

Sha W.-Y. and K.-R. Li, 1979: Relationship among subtropical high and Mei-yu in the lower Changjang valley, sea surface temperatures of Pacific Ocean. *Collected Geographical papers*, **11**, 126–137.

Wang W.-C. and K. Li, 1990: Precipitation fluctuation over semiarid region in Northern China and the relationship with El Nino/Southern Oscillation. *J. Climate*, **3**, 769–783.

Wang S.-W. and Z.-C. Zhao, 1981: Droughts and floods in China, 1470–1979, *Climate and History*, Wigley, *et al.* eds. Cambridge University Press, 271–288.

Xu G. and A. Dong, 1982: The quasi-three year period of precipitation in the west of China. *Plateau Meteorology*, **1**, 11–17 (in Chinese).

Xu G., M. Li and Z. Zhang, 1983: Seasonal variation of the rainbelts in China. *Scientia Atmospherica Sinica*, **7(3)**, 312–318 (in Chinese).

Yasunari, T., 1985: Zonally propagation modes of the global east–west circulation associated with the Southern Oscillation. *J. Meteor. Soc. Japan*, **63**, 1013–1029.

Yasunari, T., 1987: Global structure of the El Nino/Southern Oscillation Part II. Time evolution. *J. Meteor. Soc. Japan*, **65**, 81–102.

Yasunari, T., 1990: Impact of Indian monsoon on the coupled atmosphere/ocean system in the tropical Pacific. *Meteorol. Atoms. Phys.*, **44**, 29–41.

Yoshino, M. and M. Chiba, 1984: Division of China by rainfall amount and its seasonal cycle. *Geographical Review of Japan*, **57A**, 583–590 (in Japanese).

Zhao, H., 1986: A preliminary study of the characteristics of the precipitation oscillation in China. *Scientia Atmospherica Sinica*, **10**, 426–430 (in Chinese).

中国夏期降水量の年々変動の時空間構造

田　少奮
(筑波大学水理実験センター)
安成哲三
(筑波大学地球科学系)

160地点の40年間（1951–90年）の夏期（5–9月）の降水量を用いて、中国夏期降水量の年々変動の時空間構造を調べた。

まず、調和解析を行ない、各地点における降水量の年々変動の周期性を調べた。その結果、10年以下の年々変動の分散は、すべての地点において40%以上、61%の地点において70%以上が2–4年周期をもつ変動によって説明できる。特に3年周期が最も顕著であることが分かった。

次に、EOF解析を2–4年周期の変動に適応した。第1モードの空間分布は揚子江流域と中国北部との振

動の特徴を示している。第2モードの空間分布は、第1モードに比べてやや複雑であるが、おもに揚子江流域を含む広い梅雨 (Mei-yu) 地域と他の地域との振動を示している。二つのモードとも大きく振幅変調し、交互に消長する傾向を示している。第1、2モードの寄与率はそれぞれ12.8%と10.7%であり、それほど高くないが、EOF解析を行う前の降水量の合成図とそれぞれのモードの空間分布がよく似ていることから、両モードともEOF解析を行う前の降水量の変動をよく表していることが分かった。

さらに、上述の2つのモードと夏期インドモンスーンそしてENSOとの関係を調べた。第1モードは夏期インドモンスーン降水量、ENSOの指標であるSOI変動に関連していることが分かった。第1モードはインドモンスーンと同時相関が最も高い。また、第1モードはSOIを数ヶ月先行している傾向が見られる。このことは、ENSOに関連した偏差が中央アジア、インド洋域で最も早く出現するといういくつかの従来の研究結果を支持している。第2モードは、インドモンスーンやENSOとよい対応は見られない。